Chiral Symmetry Breaking in Interfacial Fluids of Achiral Molecules

Patrick B. Kohl and David L. Patrick*

Department of Chemistry, Western Washington University, 516 High St., Bellingham, Washington 98225

Received: February 26, 2001; In Final Form: June 25, 2001

Chiral symmetry breaking in a fluid of achiral molecules at a liquid−solid interface was studied using atomistic molecular dynamics simulation. The molecules were achiral in three dimensions, but left- and right-handed forms could be distinguished in the reduced symmetry environment of an interfacial fluid. The system consisted of a thick fluid film in contact with a crystalline monolayer adsorbed to a solid surface. When molecules in the crystalline monolayer were arranged in uniformly chiral configurations, a homochiral enantiomeric excess developed in the adjacent interfacial fluid. Fluid properties were characterized through measurements of chiral, nematic, ferroelectric order parameters, and diffusion coefficients, as a function of distance from the interface. The emergence of chirality is attributed to fluid layering near the solid surface, suggesting that interfacial chirality is commonplace in fluids composed of molecules with certain symmetry characteristics.

Introduction

Fluid properties near an interface often differ substantially from those in the bulk. For example, simulations[1] and experimental measurements[2] of interfacial fluids commonly show density oscillations in the first few atomic or molecular fluid layers, which arise as a consequence of constraints on molecular packing imposed by the presence of a solid wall. Fluids of nonspherical molecules often display orientational anisotropy, with molecules showing preferential polar or azimuthal orientation.[3] Fluids adsorbed to corrugated surfaces can develop in-plane translational order or epitaxy in the first one to two fluid layers.[4] Solutions may also undergo partial demixing driven by selective segregation of one component to the surface. These and related phenomena occur when some anisotropic property of the (lower symmetry) solid is partially communicated to the (higher symmetry) fluid. This paper examines communication of another property, chirality, from a solid surface to an interfacial fluid.

In certain cases, reduced dimensionality at a flat surface can lead to a breaking of chiral symmetry, causing individual achiral molecules to become chiral, or to form a chiral supramolecular pattern, or both. Chiral symmetry breaking has been studied in crystalline molecular films adsorbed on solid surfaces,[5] in Langmuir−Blodgett monolayers at air−water interfaces,[6] and more recently in the context of smectic liquid crystals (LC), which are layered fluids.[7] In many respects, interfacial fluids are nearly two-dimensional systems, with dimensionality increasing gradually to three-dimensions over a distance of a few molecular layers from the interface. Chiral symmetry breaking may occur in this transitional region as well, and if it does, fluid "chirality" would be expected to gradually diminish moving away from the surface. Here we examine this postulate through computer simulation of interfacial molecular fluids whose local chirality was characterized by a noninteger chiral order parameter.

Two-dimensional chirality is important in a number of different systems. For example, chiral surfaces formed by terminating a chiral crystal or by adsorbing a chiral film on the surface of an achiral crystal have been predicted to exhibit exceptional nonlinear optical properties[8] and have been known for nearly 70 years to display catalytic stereospecificity.[9] Recently discovered chiral smectic LC phases comprised of achiral molecules may show useful properties in optical switching and display applications and are interesting systems from a fundamental perspective.[7] Interfacial chirality is also of paramount importance in chiral chromatography and related technologies[10] and in heterogeneous enantioselective catalysis.[11]

What are the origins of chiral symmetry breaking in two-dimensions? In three-dimensions, all chiral molecules lack both an inversion center and a mirror plane, and hence the symmetry operations of reflection (σ), inversion (i), and improper rotation (S_n). Thus, all chiral molecules belong to one of the point groups: C_1 (asymmetric), C_n, D_n, T, O, or I, of which the last three rotational cubic groups are as a practical matter unlikely to be encountered.[12]

If a molecule is confined to two-dimensions, certain symmetry operations become disallowed. By the phrase "confined to two-dimensions," we mean that motion along one direction, call it the z-axis, is forbidden. A molecule confined to two-dimensions may still rotate about the z-axis and it may undergo translations in the x- and y-directions, but it may not undergo any motion (rotation or translation) that displaces some atoms in the z-direction. Following this definition, a nonplanar molecule freely diffusing across a flat surface, but able to rotate only about the surface normal, would be considered confined to two-dimensions.

The symmetry operations disallowed by two-dimensional confinement include all operations whose symmetry element(s) (point, line, or plane) lies wholly in the confinement plane, as symmetry operations involving these elements necessarily transfer some part of the molecule out of the plane or across the plane. Consequently, the emergence of chirality in two dimensions may depend on a molecule's orientation with respect to the confinement plane, as well as its symmetry point group: only if the orientation is such that the elements σ, i, and S_n *all* lie in the confinement plane (or if they are absent to begin with) will the molecule be chiral in two dimensions.

* To whom correspondence should be addressed; patrick@chem.wwu.edu

10.1021/jp010726x CCC: $20.00
Published on Web 08/02/2001

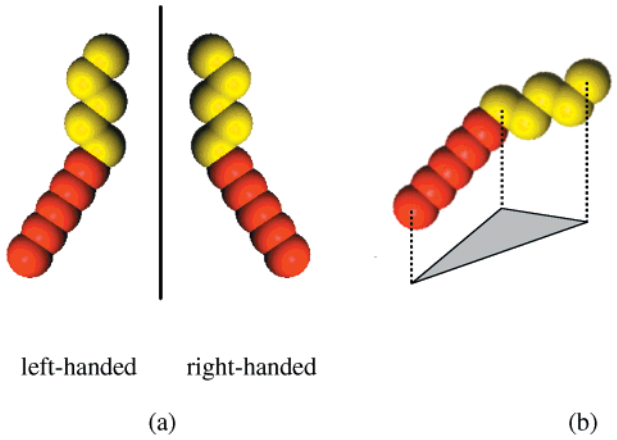

Figure 1. (a) Molecules belonging to the C_s point group are achiral in three dimensions but become chiral if the mirror plane is confined to two dimensions. The figure shows a C_s symmetry molecule simulated in this study confined to the plane of the page. It is nonsuperimposable on its mirror image unless some part is rotated out of the plane, and hence it is chiral in two dimensions. (b) The chirality parameter χ is computed from the area of the triangle formed by projecting the three atoms indicated onto the surface plane.

Using this principle, we can identify the point groups that may be chiral in two-dimensions. They include those listed above for three-dimensions, plus three more: C_{nh}, C_s, and C_i. Molecules in the C_i point group are chiral in two-dimensions regardless of their orientation, since the only requirement is that the inversion center, *i*, lie in the confinement plane. Molecules belonging to the C_{nh} and C_s point groups are chiral in two-dimensions only when oriented with their horizontal mirror plane in the in the confinement plane.[13]

We simulated films of C_s symmetry molecules, which lacked a stereocenter and hence were achiral in three dimensions. However, when properly oriented in a two-dimensional environment, the molecules display chirality, because one can distinguish between two configurations nonsuperimposable on their mirror images. This is illustrated in Figure 1a, which shows the molecule we simulated and its mirror image confined to the plane of the page. The two molecules are nonsuperimposable unless some part is rotated out of the plane. Therefore, although they lack a stereocenter in three-dimensions, they are chiral when confined as shown to two-dimensions.

Although chiral symmetry breaking has been observed in two-dimensional molecular monolayers, it remains unknown whether a similar phenomenon can occur in an interfacial fluid. To investigate this question, we performed a computer simulation study of chiral symmetry breaking among fluid molecules whose ground state conformation belonged to the C_s symmetry point group. This shape was chosen to roughly mimic 4′-octyl-4-cyanobiphenyl (8CB), an achiral molecule which has been shown in STM studies to form a single chiral monolayer on graphite.[14] When deposited onto graphite as a neat liquid, the chiral monolayer coexists with its own melt at room temperature. 8CB is probably the most widely studied molecule forming this type of solid−liquid interface.[15]

The simulations revealed the emergence of chirality in an interfacial fluid, with chiral order extending several molecular diameters into the bulk. Along with chirality, enantiomeric excess and several structural parameters of the fluid were measured in order to identify the origins of fluid chirality.

Simulation Methods

The system consisted of a fluid film 6−7 nm thick bound below by a graphite surface and above by vacuum. Molecules in the monolayer adsorbed to graphite were held frozen in one of two configurations, described below. All other molecules were treated as fully dynamic. Periodic boundaries were applied parallel to the graphite surface, resulting in simulation cells measuring 4.57 × 5.38 nm and 5.78 × 3.46 nm for the ferroelectric and antiferroelectric monolayers, respectively.

As stated above, molecular shape, internal mass distribution, and conformational flexibility were chosen to resemble the molecule 8CB, which possesses a rigid cyanobiphenyl headgroup and conformationally flexible alkyl tail. At room temperature 8CB is a bulk smectic-A LC; however, as discussed below, our model was a conventional liquid in the bulk, with a nematic order parameter less than 0.1. The rigid headgroup was constructed from five atoms arranged in a line and spaced 0.144 nm apart. The intramolecular geometry of headgroup atoms was held fixed using a combination of bond angle and distance constraints implemented using the SHAKE algorithm.[21] The mass of each headgroup atom was 35.6 amu, giving a total headgroup mass equal to that of a cyanobiphenyl moiety. The tail group was modeled as a five-atom alkane-like chain using the Ryckaert−Bellemans[16] potential function for alkane fluids. The mass of each tail atom was 14.53 amu, and the bond length for tail atoms was 0.153 nm. The equilibrium bond angle between the tail and headgroup was 109.47°, resulting in a bent conformation with a fully extended tail forming an angle of ∼147° with respect to the headgroup. Interactions between atoms in different molecules and atoms within the same molecule if separated by more than three skeletal bonds were calculated using the Lennard-Jones potential. Potential energy functions and parameters are listed in Table 1.

Two different monolayer structures were investigated: a "ferroelectric" arrangement, in which each adsorbed molecule was oriented in nearly the same direction (Figure 2a), and an "antiferroelectric" arrangement, in which molecular orientation in adjacent rows alternated by 180° (Figure 2b).[17] The two monolayers were constructed with 33 and 28 molecules, respectively. Similar domain structures have been reported in

TABLE 1: Force Field Parameters and Potential Functions

$U_{\text{dihedral}} = \sum_{i=0}^{5} a_i \cos^i(\phi)$	dihedral angle bending	$a_0 = 2.2162$ kJ/mol $a_1 = 2.9033$ $a_2 = -3.1337$ $a_3 = -0.73079$ $a_4 = 6.2673$ $a_5 = -7.5224$
$U_{\text{angle}} = \frac{1}{2} k_\theta (\theta - \theta_0)^2$	bond angle bending	$k_\theta = 126$ kJ/mol-degree^2 $\theta_0 = 109.47$ degrees
$U_{\text{bond}} = \frac{1}{2} k_r (r - r_0)^2$	bond stretching	$k_r = 310$ kJ/mol Å^2 $r_0 = 1.53$ Å
$U_{lj} = 4\epsilon\left[\left(\frac{\sigma}{r}\right)^{12} - \left(\frac{\sigma}{r}\right)^{6}\right]$	nonbonded interactions	$\epsilon = 0.143$ kJ/mol $\sigma = 3.923$ Å

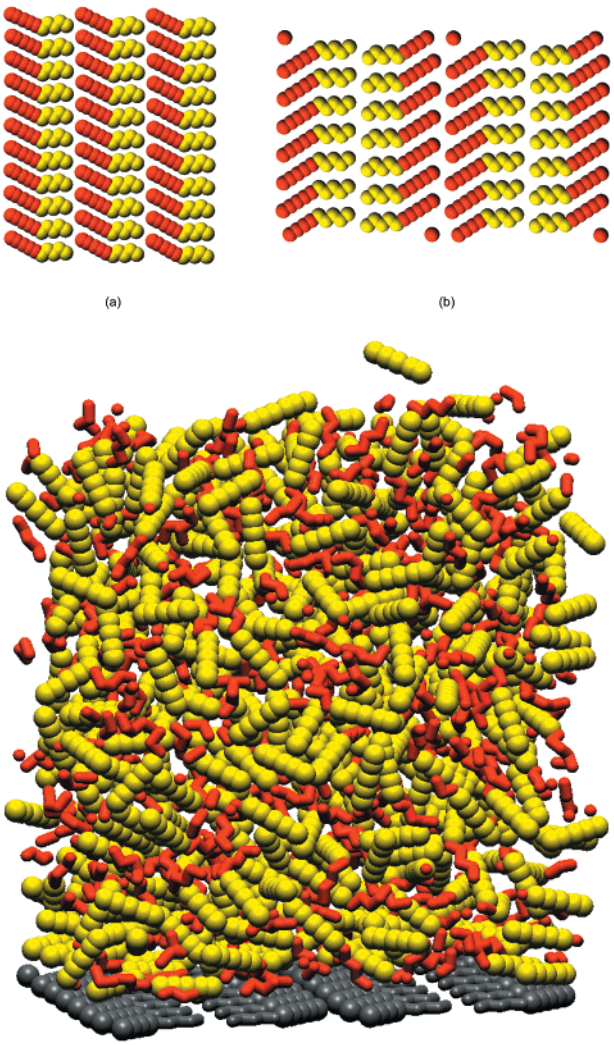

Figure 2. Two monolayer structures were used in the study, with molecules held frozen during the simulations: (a) the "ferroelectric" structure and (b) the "antiferroelectric" structure. Part (c) shows the equilibrated antiferroelectric system with its fluid film. For clarity, molecular tails in part (c) have been rendered as tubes and the atoms drawn smaller than the van der Waals radius.

STM observations of crystalline monolayers of alkylcyanobiphenyl molecules on graphite.[18] The graphite surface was modeled using the series expansion potential introduced by Steele.[19] If molecules in the first monolayer were not held fixed, they would diffuse laterally and lose some of their positional order. They do not desorb, and the overall structure remains more-or-less intact over the period covered by the simulations. However, as our focus in this study was on determining the influence of an interface on the properties of the fluid, we held the monolayer frozen to provide a well-defined and unchanging surface. The temperature of both systems was held constant at 375 K using a Berendsen thermostat,[20] which was slightly above the freezing point of the fluid (~350 K).

Molecular monolayers were prepared by performing ~5000 steps of energy minimization of a single monolayer on graphite under conditions of constant cell size. The positions and conformations of molecules did not change appreciably during minimization, but no effort was made to find a configuration that resulted in global minimization of the energy. After minimization, the monolayer was frozen and the remaining molecules introduced within the simulation cell.

Introduction of the remaining molecules was done in two steps. First, the bulk fluid was placed in a cubic simulation cell with fully periodic boundaries and equilibrated for 100 ps at 375 K. The resulting disordered liquid was then placed atop the frozen monolayer, and the entire system was equilibrated for a further 1000 ps, with periodic boundaries in the *x*- and *y*-directions only. Equilibration was followed by 5000 ps of simulation, during which structural and dynamical parameters were tabulated and averaged. A snapshot of the fully equilibrated antiferroelectric monolayer system is shown in Figure 2c. The systems contained a total of 396 and 401 molecules for the ferroelectric and antiferroelectric monolayers. Simulations were performed using a modified version of the parallel molecular dynamics package DL_POLY with a time step of 0.001 ps.[21]

Analysis Methods

We introduce here a simple geometric measure of the chirality of fluid molecules that accounts for both molecular conformation and orientation with respect to the graphite substrate (the confinement plane). The chirality of a fluid molecule can be defined as $\chi = \pm(A/A_o)$, where A is the area of the triangle whose vertices are obtained by projecting onto the surface plane both ends of the rigid headgroup and the last atom in the tail, as shown in Figure 1b. A_o was the average area so obtained for molecules in the frozen monolayer. χ was assigned a positive value if the molecule's chirality was the same as those in the monolayer (homochiral), and a negative value if it was opposite (heterochiral). The definition works equally well for molecules with any conformation and any orientation. Projected molecular area provides a suitable measure of chirality because: (1) it is a continuously varying quantity, (2) it provides an unbiased way to distinguish between molecules with similar conformations, but opposite chirality, and (3) it accounts for the impact of molecular conformation and orientation on chirality, including out-of-plane orientation. Note that this chirality measure is only meaningful in an interfacial system or layered material with two-dimensional character.

The chirality parameter, χ, was close to zero for molecules with crumpled tails and those with nearly linear conformations, since their projected areas were small. Molecules whose long axis was oriented out of the surface plane also gave small projected areas, and hence a small chirality. Molecules with the largest chirality were oriented parallel to the surface and had fully extended tails. The range of χ for fluid molecules was nearly ± 2. (The reason it was not ± 1 is as follows: Chirality is computed from the projected area of a fluid molecule, divided by the average projected area of molecules in the frozen monolayer. All molecules in the frozen monolayer have a conformation that is close to minimizing their potential energy, but molecules in the bulk fluid have a range of conformations. Some of these give a projected area larger than the projected area of frozen monolayer molecules, resulting a chirality parameter larger than one.) Because molecules in the frozen surface layer were both parallel to the surface and fully extended, χ may also be viewed as an approximate measure of the combined conformational and orientational similarity between fluid and surface molecules, where differences in orientation about the *z*-axis are disregarded.

The root-mean-squared average of molecular chirality, $\langle\chi^2\rangle^{1/2}$, is a measure of the overall chirality of a set of molecules, and the mean value, $\langle\chi\rangle$, provides a measure of enantiomeric excess. In the bulk fluid, where molecule orientations were completely random, the enantiomeric excess $\langle\chi\rangle = 0$. However $\langle\chi^2\rangle^{1/2}$ does not vanish in the bulk, but rather levels off at some constant,

positive value (in our system this constant was ~0.7). This does not mean that the bulk fluid is chiral. It results instead from the fact that the projected area A associated with a randomly oriented molecule is usually different from zero, so $\langle\chi^2\rangle^{1/2} = \langle(\pm A/A_o)^2\rangle^{1/2}$ is greater than zero. This is easily confirmed by projecting a set of randomly shaped, randomly oriented triangles onto a fixed plane. In presenting data for overall fluid chirality, we therefore subtracted the constant $\langle\chi^2\rangle^{1/2}_{\text{bulk}}$ measured for the bulk fluid.

The chirality of molecules as a function of their height above the graphite surface was measured by dividing the system into thin slices and computing over the simulation interval the time averaged chirality of all molecules whose center of mass occupied each slice. This procedure produced a set of histograms showing subpopulations of homochiral and heterochiral molecules at each height range. These histograms were then normalized by dividing by the bulk fluid distribution, giving the relative probability of observing a molecule with a certain chirality at a certain height.

Translational and orientational order in the fluid were assessed by measuring the height dependence of the fluid density and nematic order parameter. The scalar nematic order parameter, s at a height z above the substrate was defined as the largest eigenvalue of the Q-tensor

$$Q_{\alpha\beta}(z) = \frac{1}{N(z)}\sum_{i=1}^{N(z)}\left(\frac{3}{2}u_{i\alpha}u_{i\beta} - \frac{1}{2}\delta_{\alpha\beta}\right) \quad \alpha, \beta = x, y, z$$

where $N(z)$ is the number of molecules in a slice 0.1 nm thick centered at z, $u_{i\alpha}$ and $u_{i\beta}$ are components of the unit vector defining the orientation of the rigid headgroup of molecule i, and $\delta_{\alpha\beta}$ is the Kronecker delta function.[22] The nematic order parameter, s is a measure of the extent to which molecules in the fluid orient parallel to one another. It has a value between 0 and +1, with 0 representing an isotropic fluid and +1 representing a fluid with perfect uniaxial order.

For the ferroelectric monolayer system, we measured an additional order parameter, calculated as the dot product of the unit vector defining the orientation of the headgroup of a molecule in the monolayer with the unit vector for the headgroup of each fluid molecule. These values were between −1 and 1. This "ferroelectric order parameter", F, is a measure of the extent to which a particular molecule in the fluid is aligned parallel ($F = +1$), antiparallel ($F = -1$), or perpendicular ($F = 0$) to molecules in the monolayer. F was measured for every fluid molecule then tabulated into a set of histograms for each height range.

Dynamic properties of the fluid were quantified though diffusion coefficients, calculated using the Einstein relation, measured as a function of height above the surface.[23]

Results

Fluid Chirality. Overall fluid chirality, $\langle\chi^2\rangle^{1/2} - \langle\chi^2\rangle^{1/2}_{\text{bulk}}$ in the first 45 Å above the surface is shown in Figure 3. The abscissa origin is at the graphite surface, and the vacuum interface is located at 60−70 Å. For comparison, fluid density is also shown as a dashed line, plotted with an arbitrary ordinate scale. The frozen monolayer is at a height of about 4 Å, and the first fluid layer is centered at about 7 Å. The chirality plots show a set of 3−4 oscillations, decaying in amplitude with increasing distance from the surface. These oscillations correspond to regions of nonzero chirality in the fluid. Note that the peak centers generally coincide with the positions of density maxima, indicating that molecules near the center of the fluid layers are most chiral. Chirality is low in the intralayer regions

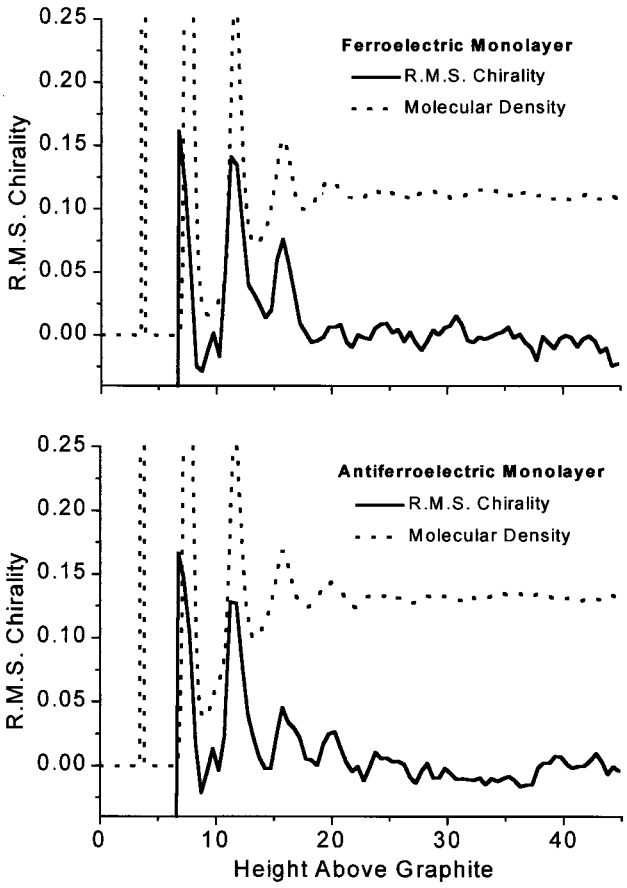

Figure 3. The root-mean-squared chirality $\langle\chi^2\rangle^{1/2} - \langle\chi^2\rangle^{1/2}_{\text{bulk}}$ for fluid molecules near the graphite surface shows an oscillatory pattern. Chirality is plotted as a solid line, with fluid density (dashed line) provided for reference (plotted with an arbitrary ordinate scale). Peaks correspond to regions of high fluid chirality. The graphite surface is located at $h = 0$ and the frozen monolayer is located at $h \approx 4$ Å.

because molecules at those heights tended to orient with a large out-of-plane component. We observe that variations in fluid chirality closely resemble the density oscillations, both in the rate of decay and overall shape. This correspondence agrees with the expectation that regions of higher layer confinement, and hence larger and sharper density oscillations, will produce higher chirality. Also note that the plots for the two systems do not differ significantly within the level of statistical noise, indicating that overall chirality was insensitive to the structure of the frozen monolayer.

Further insight into fluid chirality comes from examination of individual subpopulations of chiral molecules, shown in Figure 4. The histograms in the upper half of the figure show the distribution of molecular chirality at regions within the first fluid layer, while those in the lower half show fluid chirality at more widely spaced intervals further into the bulk. The histograms for the first layer reveal two primary populations of molecules: one homochiral and one heterochiral. The achiral population ($\chi \sim 0$) was suppressed by layer confinement, since rotation out of the surface plane is one of the principal ways molecules achieve low chirality. The homochiral population was larger than the heterochiral one in both systems, leading to an enantiomeric excess at the interface. This excess was most pronounced above the antiferroelectric monolayer (see below). Further from the surface, in the region between the first and second fluid layers, the homo- and heterochiral populations became equal, and a significant number of achiral molecules

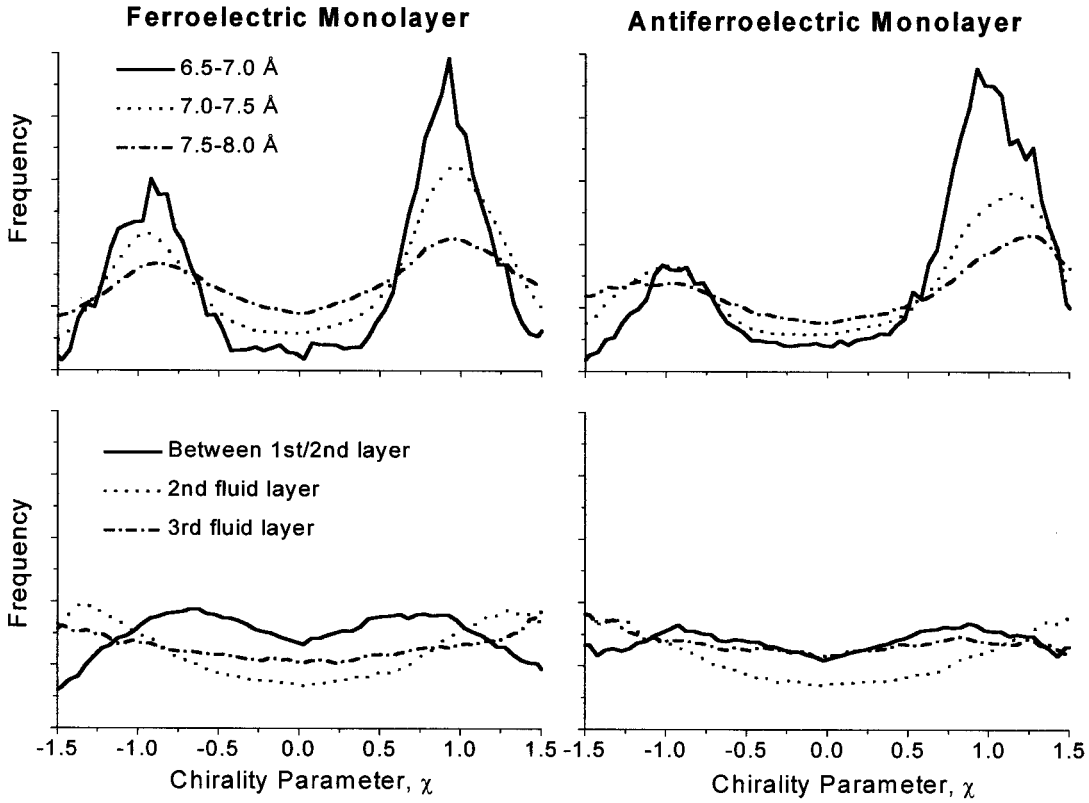

Figure 4. The histograms show probability distributions for observing different values of molecular chirality at various heights above the surface. The upper panels represent regions within the first fluid layer, and the lower panels represent regions further from the surface. Results from the ferroelectric monolayer system are shown on the left, and results from the antiferroelectric system are shown on the right. Each curve was normalized by dividing by the bulk distribution.

began to appear. In the second and third fluid layers, the distributions continued to evolve toward that of the bulk, and by the fourth or fifth fluid layer (not shown) the transition was complete.

Enantiomeric excess, $\langle\chi\rangle$ is plotted in Figure 5, with fluid density again shown as a dashed line. A statistically significant excess of homochiral molecules was observed in the leading half of the fluid layer closest to graphite in both systems. The effect was more pronounced above the antiferroelectric monolayer, but in both systems it exceeded the level of statistical noise, judged from fluctuations in $\langle\chi\rangle$ measured far from the surface. The maximum value for $\langle\chi\rangle$ was 0.08 above the ferroelectric monolayer, and 0.29 above the antiferroelectric monolayer. The ferroelectric system also showed one data point closest to the frozen monolayer indicating heterochiral excess (i.e., a negative value for $\langle\chi\rangle$). However, this point corresponds to a region with a density 1/700th of the bulk fluid (more than an order of magnitude smaller than any other measured point), and so we ascribe it to noise arising from undersampling.

Fluid Density. The dashed lines in Figures 3 and 5 show variations in the density of the molecules' center of mass as a function of height. The oscillatory pattern is similar to that seen in other interfacial fluids.[1] These effects and others are illustrated more clearly in Figure 6, which plots separately the density of headgroup and tailgroup atoms. Several features are noteworthy. First, except in the first fluid layer, the density maxima for head and tail atoms do not coincide exactly, but are shifted relative to one another by 0.024 nm, or 6% of the mean interlayer spacing. Peaks associated with head atoms are also sharper than those of the tail. Peak width is inversely proportional to the extent of positional disorder, which near the graphite wall was greater among tail atoms than among head atoms. This difference can be understood in terms of the relative conformational flexibility of head and tail groups: confinement of the flexible molecular tails to two dimensions incurs a greater loss of configurational entropy than does confinement of the rigid headgroups, and so the tails are less well positionally ordered. The fluid−vacuum interface was quite diffuse, extending over a region of ~1 nm. There was no layering at this interface, nor any discernible enrichment of headgroup or tailgroup atoms. Comparison of the two systems shows that the structure of the frozen monolayer had little effect on fluid density.

Nematic Order. Figure 7 shows the height dependence of the nematic order parameter. In both systems, orientational order was highest near the frozen monolayer, decaying to a bulk value of $s \sim 0.25$ by the beginning of the third fluid layer. This value is higher than the average nematic order parameter measured in bulk simulations with fully periodic boundaries ($s = 0.08$). The discrepancy results from artificially dividing the system into thin slabs in order to calculate the height dependence of the order parameter, which leads to an overestimation of nematic order.[24] Based on simulations using fully periodic boundaries in which the cell was not divided into thin slices, it was clear that this model does not form a bulk LC phase, despite the high nematic order parameter near the interface.

The ferroelectric monolayer system displayed marginally higher nematic order in the first and second fluid layers. It is notable, however, that this did not coincide with increased fluid chirality or with a larger enantiomeric excess of homochiral fluid molecules (viz. Figures 3 and 5). Visual inspection of snapshots taken throughout the simulations also showed that the first fluid layer in both systems exhibited strong in-plane density oscillations parallel to the nematic director, with density maxima centered above molecules in the frozen monolayer. In

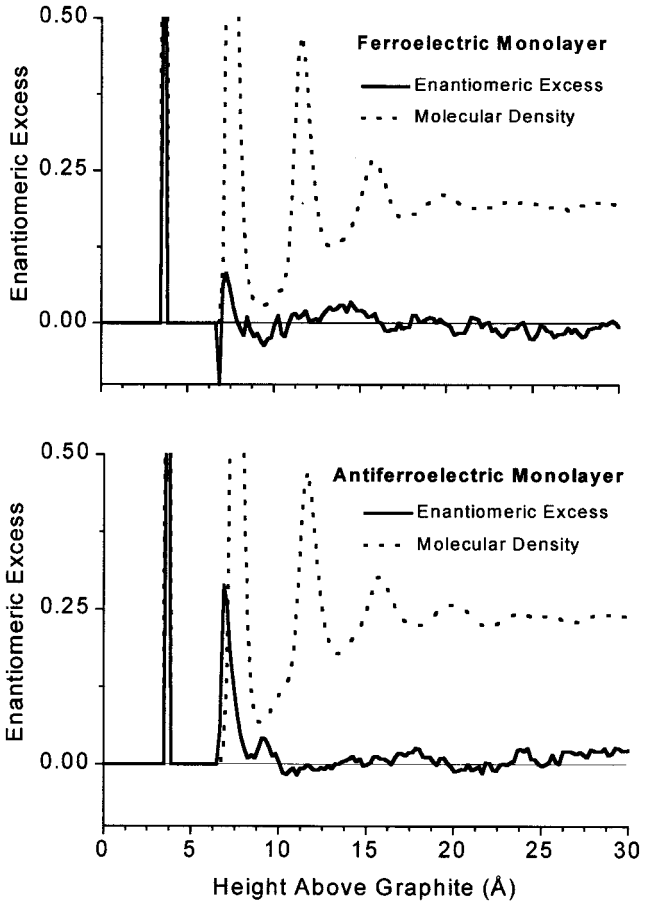

Figure 5. A significant enantiomeric excess, $\langle\chi\rangle$, was observed in the leading edge of the first fluid layer in both systems. Positive values indicate a homochiral excess. Fluid density is shown for comparison, plotted with an arbitrary ordinate scale. The graphite surface is located at $h = 0$, and the frozen monolayer is located at $h \approx 4$ Å.

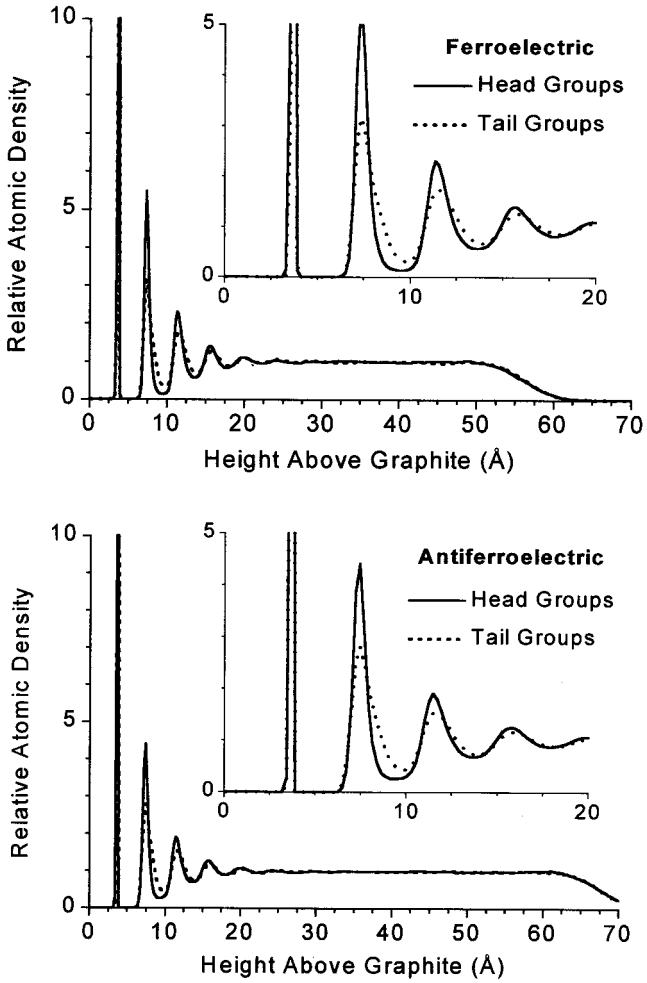

Figure 6. The density of molecular headgroup atoms (solid lines) and tailgroup atoms (dashed lines) displayed an oscillatory pattern near the graphite wall, indicating strong fluid layering. Insets show details of these oscillations in the first 20 Å. Oscillations were followed by a region of bulk fluid 30−40 Å thick. The vacuum interface was located at $z \approx 60$ Å in the ferroelectric system and $z \approx 70$ Å in the antiferroelectric system. The graphite surface is located at $h = 0$, and the frozen monolayer is located at $h \approx 4$ Å.

other words, molecules in the first fluid layer were arranged similarly to those in the frozen monolayer, forming a nearly epitaxial fluid (see Figure 9). Density oscillations parallel to the nematic director are a characteristic of smectic LCs. Thus, over a distance of just four molecular layers, the structure evolves from crystalline → smectic LC → nematic LC → isotropic. The sharp peak at the leading edge of the first fluid layers in both graphs is an artifact of the extremely low density at those data points.

Ferroelectric Order. The ferroelectric order parameter measured at various heights above the ferroelectric monolayer is shown in Figure 8. It quantifies orientational similarity between fluid and surface molecules. In the first fluid layer (upper panel), molecules overwhelmingly oriented either parallel or antiparallel to those in the monolayer, as witnessed by large populations at extreme values of the ferroelectric order parameter. Other orientations were almost completely suppressed. In this region, very close to the surface, the parallel population was much more sharply peaked than the antiparallel population, and contained a greater number of molecules. This asymmetry in the histogram, combined with a high nematic order parameter, means the first fluid layer possessed unidirectional (polar) symmetry, similar to (but not as pronounced as) the frozen monolayer.

The ferroelectric order parameter between the first and second fluid layers was qualitatively different from within the layers, as shown by the dashed line in the upper panel of Figure 8. The distribution tended toward lower overall ferroelectric order (peak centers shifted from ± 1 to ± 0.8), and became symmetric (uniaxial, rather than unidirectional fluid symmetry). The shift in peak centers occurred because intralayer molecules were frequently oriented out of the surface plane, spanning two or more layers. Fluid uniaxiality persisted until about the fourth fluid layer, gradually becoming less pronounced with increasing distance from the interface. The bulk distribution was a flat line.

Molecular Diffusion. The diffusion data for the two systems (not shown) were very similar and rather typical of interfacial fluids. The mean diffusion coefficient in the first fluid layer was 6.3×10^{-6} cm^2 s^{-1}, high enough to indicate a fluid phase. Diffusion increased sharply at the second fluid layer and continued in a linear progression into the bulk. Diffusion near the liquid/solid interface was dominated by motion approximately parallel to the nematic director. Near the surface, in-plane motion was 5−10 times greater than motion along the surface normal. The height dependence of diffusion coefficients was determined by assigning molecules to 5 Å bins, according to the position of their center of mass. Because molecules were in motion, these assignments were periodically retabulated at intervals much smaller than the mean interbin transit time.

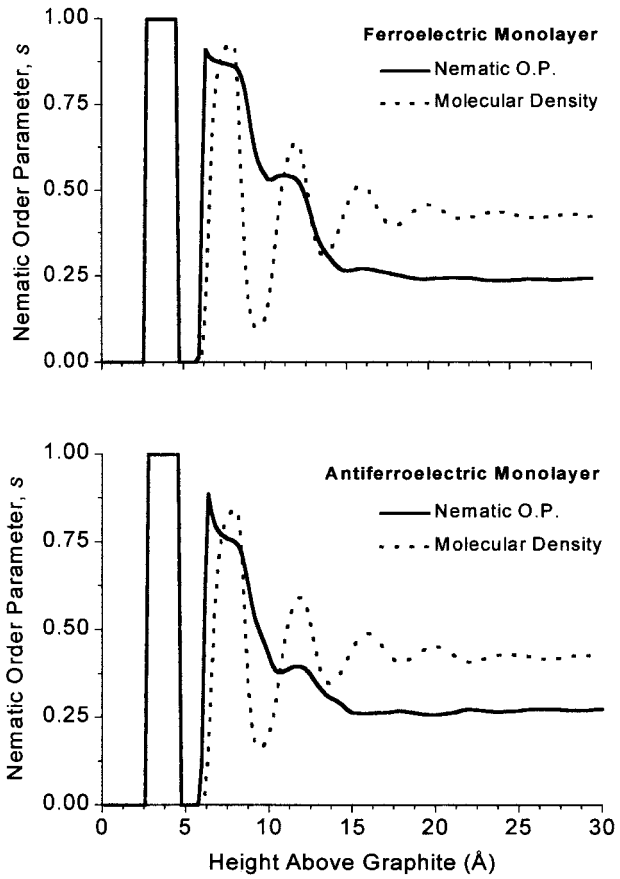

Figure 7. The fluid showed strong in-plane orientational order in the first two layers, but by the third layer the nematic order parameter had decayed to its bulk value. The method used to calculate s resulted in an overestimation (refer to text); simulations using fully periodic boundaries gave a bulk nematic order parameter $s \sim 0.08$, indicating a nearly isotropic fluid. The graphite surface is located at $h = 0$, and the frozen monolayer is located at $h \approx 4$ Å.

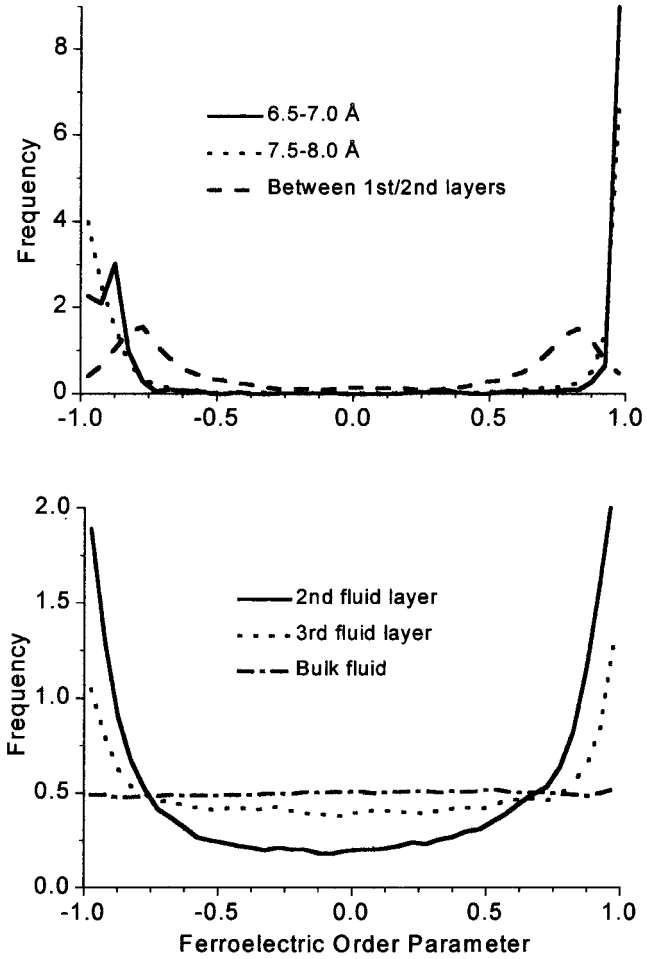

Figure 8. The ferroelectric order parameter is a measure of the extent to which fluid molecules oriented parallel (+1) or antiparallel (-1) to molecules in the monolayer. The data were measured above the ferroelectric monolayer. The upper panel shows regions close to the graphite surface, and the lower panel shows regions further into the bulk liquid.

Discussion

These results demonstrate that the interfacial fluid is chiral and that this chirality as measured by the parameter $\langle\chi^2\rangle^{1/2}$ decays into the bulk over a distance of 3−4 fluid layers. There exists moreover an enantiomeric excess of homochiral molecules in the first fluid layer, the extent depending on monolayer structure. Here we shall discuss the relationship between this chirality and other elements of fluid and monolayer molecular order.

Based on arguments presented in the Introduction, in-plane confinement of the molecule's C_s mirror plane should by itself be sufficient to produce chirality, and so a similar fluid film adsorbed to a perfectly smooth surface would also be expected to break chiral symmetry. Indeed, Figure 3 shows that differences in the structure of the frozen monolayer had little or no impact on overall fluid chirality. Likewise, nematic order does not appear to be necessary for fluid chirality, as the data demonstrate in two ways: First, s had decayed to its bulk value by the beginning of the third fluid layer, while chirality persisted into the third or fourth layers. Second, although nematic order was greatest above the ferroelectric monolayer system, rms chirality was essentially indistinguishable from the antiferroelectric system. Fluid chirality also showed little correlation to ferroelectric order. The ferroelectric order parameter data show that fluid layers with either polar or uniaxial symmetry can be chiral, and, like s, the ferroelectric order parameter had nearly decayed to its bulk distribution in fluid regions where chirality still persisted. We conclude that the emergence of chirality in this type of fluid can be singularly attributed to layer confinement (or density oscillations).

In the absence of a further reduction in symmetry, a film adsorbed to a smooth wall would be racemic. We have seen that the frozen chiral monolayer can break racemic symmetry, leading to a homochiral excess in the first fluid layer. This further symmetry breaking occurred above both monolayer structures and was stronger in the antiferroelectric system (although it did not penetrate any further into the fluid). Examination of snapshots showing molecules in the region of homochiral excess indicated that in order to approach close to the surface, fluid molecules had to adopt nearly the same conformation as molecules in the monolayer and to "nestle" into one of the grooves between frozen molecules. Thus, the molecules that contributed most to enantiomeric excess were those which were most nearly epitaxial to the frozen monolayer. Molecules in the first fluid layer that were slightly further from the surface were less constrained by epitaxy and consequently showed less enantiomeric excess, despite possessing significant chirality.

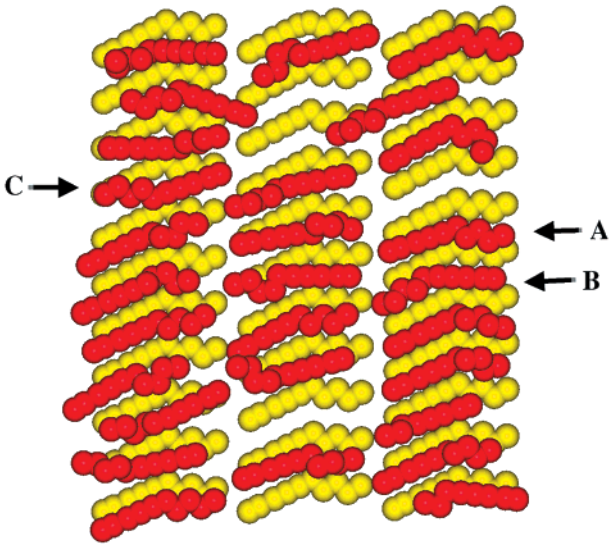

Figure 9. The figure shows a snapshot of the ferroelectric monolayer and first fluid layer. Three types of molecules are labeled with arrows: (A) parallel and homochiral; (B) antiparallel and heterochiral; (C) antiparallel and homochiral. Note that molecules possessing configurations similar to (A) or (B) conform more closely to the shape of grooves between molecules in the frozen monolayer. Molecules tended to adopt one of these two configurations, with configuration (A) slightly favored over configuration (B).

TABLE 2: Molecular Configuration Statistics in the Ferroelectric System

	homochiral	heterochiral
parallel orientation	43%	13%
antiparallel orientation	13%	31%

To gain further insight into this issue, we labeled molecules in the first fluid layer as being either homochiral or heterochiral, and also as being oriented either substantially parallel or antiparallel to molecules in the frozen monolayer. The small number of molecules with ambiguous chirality or orientation were not included. The results are summarized in Table 2 using data from the ferroelectric system. They reflect the homochiral excess of the first fluid layer (56% homochiral vs 44% heterochiral), as well as its uniaxial symmetry (56% parallel vs 44% antiparallel). In addition, they show a strong positive correlation between chirality and ferroelectric order; fluid molecules that oriented parallel to those in the frozen monolayer (positive ferroelectric order parameter) were overwhelmingly homochiral, and those that oriented antiparallel were overwhelmingly heterochiral. This correlation results from fluid epitaxy. In order for a fluid molecule to align in registry with the frozen monolayer, it must adopt either a parallel/homochiral configuration or an antiparallel/heterochiral configuration, with the former being slightly preferred. Any other configuration forces part of the molecule out of the intermolecular grooves in the frozen monolayer. Several examples are shown in Figure 9, which is a snapshot of the frozen monolayer and first fluid layer in the ferroelectric system. Arrows indicate representative molecules with different configurations. The molecule denoted "A" (parallel and homochiral), and the molecule denoted "B" (antiparallel and heterochiral) are able to conform more closely to the shapes of the grooves between molecules in the frozen monolayer than fluid molecules with other configurations, such as the one denoted "C" (antiparallel and homochiral). It is clear that the occurrence of an enantiomeric excess is very sensitive to the structural details of the solid surface and is therefore likely to differ significantly between systems.

Research on a number of subjects, from chiral crystal growth to the origins of homochirality in living systems, seeks to understand how chiral preferences are communicated between different components of a heterogeneous system and how small chiral perturbations can lead to large-scale enantiomeric excess. In the simulations, the size of these perturbations is readily calculated as a free energy difference, ΔG, between homochiral and heterochiral molecules arising from the proximity of the solid wall. ΔG is computed from the relative numbers of homochiral and heterochiral molecules:

$$\Delta G = -kT \ln(P_{\text{homo}}/P_{\text{hetero}})$$

where P_{homo} and P_{hetero} are the probabilities of observing homochiral and heterochiral molecules at a particular height above the surface, and $\Delta G = G_{\text{homo}} - G_{\text{hetero}}$ is the free energy difference of the two configurations. The probabilities are found by separately integrating the homochiral and heterochiral peak areas in Figure 4. Performing the calculation for molecules in the region of strongest homochiral excess ($z = 6.5-7.0$ Å) gives $\Delta G = -0.35\ kT$, or $-7.6\ \epsilon$ for the ferroelectric system, and $\Delta G = -1.1\ kT$, or $-24\ \epsilon$ for the antiferroelectric system, where ϵ is the Lennard-Jones well depth. Viewed in terms of free energy, the homochiral influence of the antiferroelectric monolayer was more than three times greater than the ferroelectric one.

The effects of changes in temperature and the molecular mechanics force field were not investigated in this work, but one can make some deductions about their likely importance based on the findings reported above. Chirality and enantiomeric excess are aspects of fluid structure, arising from layering and epitaxy, respectively. The gross structural features of interfacial fluids are dominated by entropic factors (not energetic factors), so the most important parameters are likely to be those that alter the contribution of entropy to the system free energy. Thus small changes in system parameters such as the van der Waals interaction strength, ϵ, or atomic radii are unlikely to be very important. Indeed, even fluids composed of hard spheres (which have no attractive interactions) develop structure at an interface.[1] Conversely, parameters such as temperature or the number and position of flexible units in a molecule may be very important, as these directly affect entropy.

Conclusions

We have observed chiral symmetry breaking in a fluid of achiral molecules at two solid−liquid interfaces. This chirality extended ~20 Å or 3−4 liquid layers away from the surface. Examination of a variety of fluid structural parameters led to the conclusion that chiral symmetry breaking occurs as a result of layer confinement and is largely independent from other aspects of molecular order. Since density oscillations appear to be a common feature of interfacial fluids, near-surface chirality may be widespread in fluid systems with molecules of appropriate symmetry. A significant homochiral excess was also observed in the first fluid layer, which, unlike overall chirality, appears to be strongly dependent on the structure of the surface monolayer.

Acknowledgment. We thank B. Purnell for his assistance. This work was supported by a Cottrell College Science Award from Research Corporation (CC4564) and the National Science Foundation (CAREER/PECASE Program CHE-9985428). P. K. thanks The Council on Undergraduate Research for providing a summer research fellowship.

References and Notes

(1) Henderson, D.; Abraham, F. F.; Barker, J. A. *Mol. Phys*. **1976**, *31*, 1291.

(2) Yu, C.-J.; Richter, A. G.; Datta, A.; Durbin, M. K.; Dutta, P. *Phys. Rev. Lett*. **1999**, *82*, 2326.

(3) Xia, T. K.; Ouyang, J.; Ribarsky, M. W.; Landman, U. *Phys. Rev. Lett*. **1992**, *69*, 1967.

(4) Rhykerd, C. L., Jr.; Schoen, M.; Diestler, D. J.; Cushman, J. H. *Nature* **1987**, *330*, 461.

(5) (a) Eckhardt, C. J.; Peachey, N. M.; Swanson, D. R.; Takacs, J. M.; Kahn, M. A.; Gong, X.; Kim, J.-H.; Wang, J.; Uphaus, R. A. *Nature* **1994**, *368*, 440. (b) Lopinksi, G. P.; Moffatt, D. J.; Wolkow, D. D. M. *Nature* **1998**, *392*, 909. (c) Charra, F.; Cousty, J. *Phys. Rev. Lett*. **1998**, *80*, 1682. (d) Fang, H.; Giancarlo, L. C.; Flynn, G. W. *J. Phys. Chem. B* **1998**, *102*, 7311.

(6) Viswanathan, R.; Zasadzinski, J. A.; Schwartz, D. K. *Nature* **1994**, *368*, 440.

(7) (a) Link, D. R.; Natale, G.; Shao, R.; Maclennan, J. E.; Clark, N. A. Korblöva, E.; Walba, D. M. *Science* **1997**, *278*, 1924. (b) Walba, D. M.; Körblova, E.; Shao, R.; Maclennan, J. E.; Link, D. R.; Glaser, M. A.; Clark, N. A. *Science* **2000**, *288*, 2181. (c) Pratibha, R.; Madhusudana, N. V.; Sadashiva, B. K. *Science* **2000**, *288*, 2184.

(8) Hecht, L.; Barron, L. *Chem. Phys. Lett.* **1994**, *225*, 525.

(9) Rodolph, L. *Naturwissenschaften* **1932**, *20*, 363.

(10) Sheldon, R. A. *Chirotechnology*; Marcel Dekker: NY, 1993.

(11) Wan, T. A.; Davies, M. E. *Nature* **1994**, *370*, 449.

(12) Carter, R. L. *Molecular Symmetry and Group Theory*; John Wiley and Sons: New York, 1998.

(13) From this it also follows that a molecule that is chiral in m dimensions will always be chiral in n dimensions if $n \leq m$.

(14) Foster, J. S.; Frommer, J. E. *Nature* **1988**, *333*, 542.

(15) See for example, Patrick, D. L.; Cee, V. J.; Beebe, T. P., Jr. *J. Phys. Chem*. **1996**, *100*, 8478 and references therein.

(16) Ryckaert, J. P.; Bellemans, A. *Discuss. Faraday Soc*. **1978**, *66*, 95.

(17) The terms ferroelectric and antiferroelectric are descriptive of the type of orientational order only. No electrostatic terms were used in the force field.

(18) Patrick, D. L.; Beebe, T. P., Jr. *Langmuir* **1994**, *10*, 298.

(19) (a) Steele, W. A.; *Surf. Sci.* **1973**, *36*, 317. (b) Steele, W. A.; Vernov, A. V.; Tildesley, D. J. *Carbon* **1987**, *25*, 7.

(20) Berendsen, H. J. C.; Postma, J. P. M.; van Gunsteren, W. F.; DiNola, A.; Haak, J. R. *J. Phys. Chem*. **1984**, *81*, 3684.

(21) Forester, T. R.; Smith, W. Daresbury Laboratory, U.K.

(22) De Miguel, E.; Rull, L. F.; Challam, M. K.; Gubbins, K. E. *Mol. Simul*. **1991**, *7*, 357.

(23) Allen, M. P.; Tildesley, D. J. *Computer Simulation of Liquids*; Clarendon Press: Oxford, 1987.

(24) Wall, G. D.; Cleaver, D. J. *Phys. Rev. E* **1997**, *56*, 4.